Electronic supplementary information

Proposed Mechanical Method for Switching Spin Transport Channel in Two-Dimensional Magnetic Metal-Magnetic Semiconductor Van der Waals Contacts

Pengfei Gao, Xingxing Li and Jinlong Yang**

Department of Chemical Physics, Hefei National Laboratory for Physical Sciences at the Microscale, and Synergetic Innovation Center of Quantum Information & Quantum Physics, University of Science and Technology of China, Hefei, Anhui 230026, China.

**Email: lixx@ustc.edu.cn; jlyang@ustc.edu.cn*

Computational Methods

First principles calculations are performed by Vienna ab initio simulation package (VASP) [1]with van der Waals interaction (vdW) correction using the DFT-D3 method.[2,3] The generalized gradient approximation (GGA) with Perdew-Burke-Ernzerhof (PBE) functional[4] is used to describe the exchange and correlation interaction. The PBE+U method[5] is used to treat the strong-correlation effect of transition metal's 3d electrons. A typical effective Hubbard U_{eff} of 3.0 eV for 3d orbital is added for both the Cr-3d and Fe-3d orbitals. The projector augmented wave (PAW) potential[6] and the plane-wave cut-off energy of 400 eV are used. A Monkhorst-Pack k-point mesh[7] of 9 × 9 × 1 is used and a 15 Å vacuum layer is introduced between the repeated slabs along the z-direction. Dipole correction is applied. The criterion for the total energy is set as 1×10^{-6} eV. The optimized monolayer lattices and experimentally measured bulk lattices of $CrGeTe_3$, CrI_3 and Fe_3GeTe_2 are listed in Table S1. The van der Waals contacts are constructed by matching unit cells of magnetic semiconductors $CrGeTe_3/CrI_3$ to ($\sqrt{3} \times \sqrt{3}$) supercells of magnetic metal Fe_3GeTe_2. The optimized lattice constant of Fe_3GeTe_2 is adopted as the lattice constants of contacts. Test calculations shows that the magnetic ground states of A- and B-stacking $Fe_3GeTe_2/CrGeTe_3$ do not change when the lattice varies from 6.82 Å (the lattice of $CrGeTe_3$) to 7.08 Å ($\sqrt{3}$ times the lattice of Fe_3GeTe_2), as shown in Table S2. The lattice mismatches are listed in Table S3. To obtain 2D interfacial sliding potential energy surface, we choose 12 × 12 grid points to perform the lateral slide of the semiconductor. The X, Y coordinates of all atoms are fixed at each grid point with the Z coordinates optimized until the forces are less than 0.02 eV/Å. We calculated the electronic structures of the metastable A-stacking and B-stacking after reoptimizing the structures without any constraint until all forces are less than 0.01 eV/Å.

To check the effect of SOC on magnetic ground states for A- and B-stacking $Fe_3GeTe_2/CrGeTe_3$, the interlayer exchange energies (E(FM)-E(AFM) per supercell) under different U values with SOC (without SOC) are calculated in Table S4. Qualitatively, SOC does not change the magnetic ground states. As long as the effective U of Fe is greater than 1 eV, the magnetic ground state keeps as AFM for A-stacking and FM for B-stacking, whether or not SOC is considered. Then we tested the effect of SOC on the electronic bands of $Fe_3GeTe_2/CrGeTe_3$. As shown in Figure S4, the electronic bands with PBE + U + SOC is very similar to the PBE + U bands presented in the article, and no obvious gap (Schottky barrier) is opened around the Fermi level by SOC.

To test the effect of U values, we calculated the interlayer exchange energies E_{ex} (E(FM)-E(AFM) per supercell) under different U values in Table S4, and the Schottky barriers in Table

S5 for A- and B-stacking $Fe_3GeTe_2/CrGeTe_3$. When the effective U of Fe_3d is greater than 1 eV, the magnetic ground state keeps as AFM for A-stacking and FM for B-stacking, and the two structures retain ohmic contacts or just have small Schottky barriers (< 0.05 eV).

To check the reliability of PBE+U functional, we further performed calculations with the more accurate hybrid HSE06 functional. The interlayer exchange energy with HSE06 for A- and B-stacking $Fe_3GeTe_2/CrGeTe_3$ is 17 meV and -16 meV, respectively. That is, A-stacking prefers AFM and B-stacking prefers FM couplings, which is qualitatively consistent with PBE+U calculations. Moreover, the projected density of states (PDOS) of A- and B-stacking structures with HSE06 are calculated, as shown in Figure S5. For A(B)-stacking, the Fermi level crosses the down (up) spin channel conduction band edges of $CrGeTe_3$, indicating a single spin channel ohmic contact reversable between A- and B-stacking, which is consistent with our conclusion in the manuscript.

Above all, SOC, U values (U(Fe_3d) > 1 eV) and HSE06 functional do not qualitatively alter the ground states and electronic properties of $Fe_3GeTe_2/CrGeTe_3$ contact, and the conclusion in the manuscript remains unchanged.

Figures S1-S5

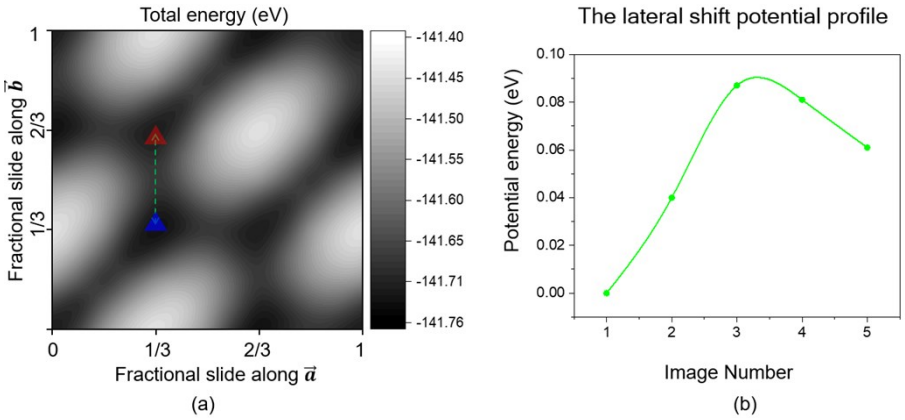

Figure S1. (a)The lateral sliding potential energy surface with AFM interlayer coupling, the red and blue triangles represent metastable A-stacking and B-stacking patterns. The abscissa and ordinate stand for the fractional shift of the $CrGeTe_3$ layer in the $\vec{a}$ and $\vec{b}$ directions of the superlattice, respectively. (b) The minimum energy pathway of sliding from B-stacking to A-stacking for $Fe_3GeTe_2/CrGeTe_3$ contact at FM state.

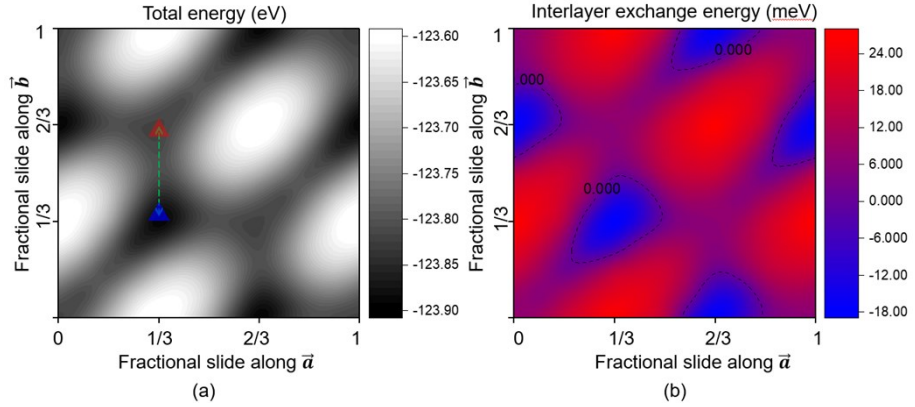

Figure S2. (a) The lateral sliding potential energy surface of Fe_3GeTe_2/CrI_3 with FM interlayer coupling. The red and blue triangles represent metastable A-stacking and B-stacking patterns, respectively. (b) 2D map of interlayer exchange energy as a function of fractional lateral slide. The abscissa and ordinate stand for the fractional shift of the CrI_3 layer in the $\vec{a}$ and $\vec{b}$ directions of the superlattice, respectively. Red (positive values) and blue colors (negative values) indicate AFM and FM coupling, respectively.

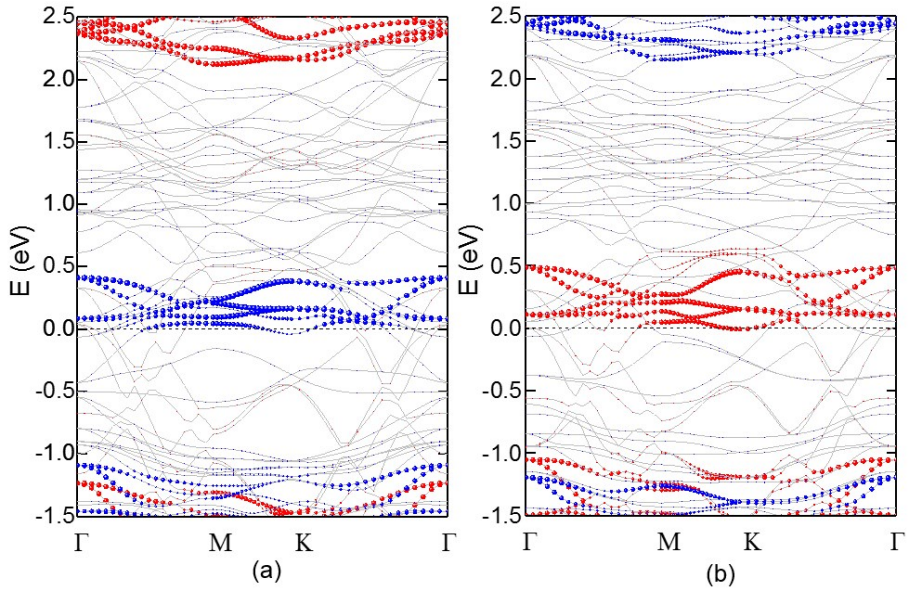

Figure S3. The electronic structure of Fe_3GeTe_2/CrI_3 contact. (a) and (b) are the projected electronic bands of A-stacking and B-stacking, respectively. The gray lines represent the bands of the whole contact. The red (blue) circles represent the up (down) spin bands of magnetic semiconductor CrI_3. The Fermi levels are set to zero.

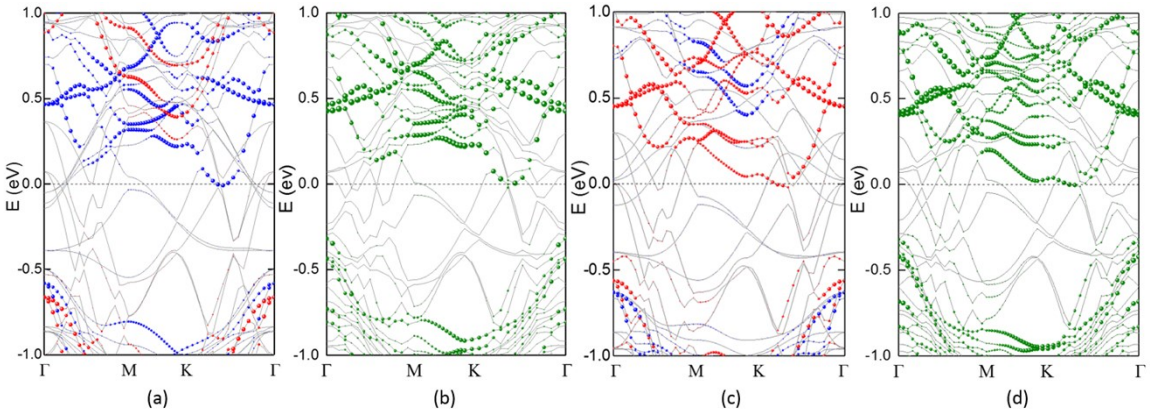

Figure S4. Electronic band structures of $Fe_3GeTe_2/CrGeTe_3$ contact. (a) and (b) are the PBE + U (U_{eff} = 3 eV) projected electronic bands without and with SOC for A-stacking structure. (c) and (d) are those for B-stacking structure. In (a) and (c) without SOC, the gray lines represent the bands of the whole contact, while the red (blue) circles of (a) and (c) represent the spin up (down) bands of magnetic semiconductor $CrGeTe_3$. In (b) and (d) with SOC, the green circles

represent the spin mixed bands of magnetic semiconductor $CrGeTe_3$. The Fermi levels are all set to zero.

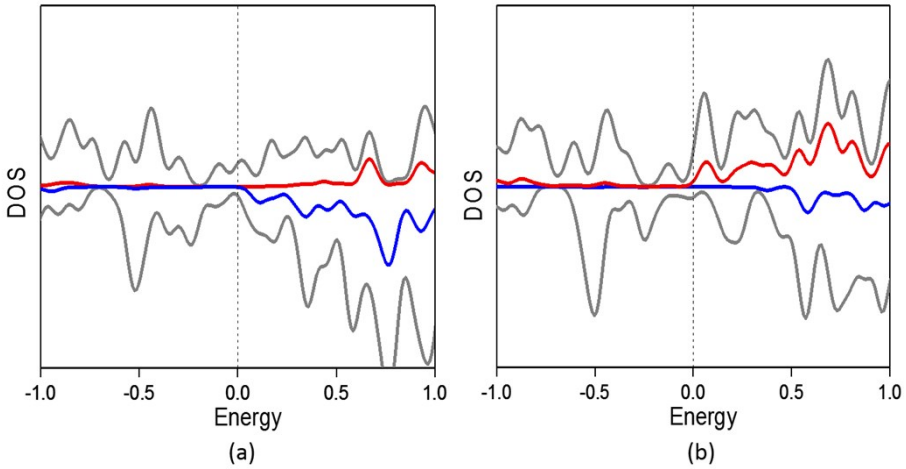

Figure S5. (a) and (b) are the projected density of states (DOS) of A- and B-stacking $Fe_3GeTe_2/CrGeTe_3$ contact with HSE06 functional. The gray lines represent the total DOS of the contact. The red (blue) line represents the spin up (down) projected DOS of magnetic semiconductor $CrGeTe_3$.

Table S1. The optimized monolayer lattice constants (Å) and experimentally measured bulk lattices (Å) of $CrGeTe_3$, CrI_3 and Fe_3GeTe_2.

	lattice (opt)	lattice (exp)
$CrGeTe_3$	6.84	6.82 [ref.8]
CrI_3	6.90	6.90 [ref.9]
Fe_3GeTe_2	4.09	4.00 [ref.10]

Table S2. The change of the E(FM), E(AFM) (eV) and interlayer exchange energy E_{ex} (meV) with the supercell lattice constant (Å) for (a) A- and (b) B-stacking $Fe_3GeTe_2/CrGeTe_3$ contact.

(a)

Lattice	6.81	6.89	6.96	7.03	7.10
E(FM)	-141.372	-141.639	-141.782	-141.804	-141.724
E(AFM)	-141.398	-141.659	-141.798	-141.820	-141.741
E_{ex}	26	20	16	16	17

(b)

Lattice	6.81	6.89	6.96	7.03	7.10
E(FM)	-141.465	-141.715	-141.850	-141.872	-141.787
E(AFM)	-141.457	-141.698	-141.827	-141.845	-141.757
E_{ex}	-8	-17	-23	-27	-30

Table S3. The lattice mismatches of van der Waals contacts $Fe_3GeTe_2/CrGeTe_3$ and Fe_3GeTe_2/CrI_3.

	Lattice mismatch
$Fe_3GeTe_2/CrGeTe_3$	3.4%
Fe_3GeTe_2/CrI_3	2.6%

Table S4. Interlayer exchange energy (E(FM)-E(AFM) per supercell) (meV) calculated using PBE + U functional with (without) SOC for (a) A-stacking and (b) B-stacking $Fe_3GeTe_2/CrGeTe_3$ with different U_{eff} values (eV) of Cr_3d and Fe_3d.

(a)

Fe\Cr	1	2	3	4
1	-5 (-7)	-4 (-6)	0 (-1)	3 (0)
2	3 (2)	6 (3)	8 (4)	11 (6)
3	4 (5)	12 (9)	15 (11)	20 (13)
4	10 (6)	16 (14)	17 (15)	22 (18)

(b)

Fe\Cr	1	2	3	4
1	69 (101)	63 (96)	58 (91)	54 (87)
2	-31 (-42)	-32 (-30)	-34 (-31)	-34 (-32)
3	-62 (-54)	-61 (-46)	-61 (-44)	-61 (-54)
4	-143 (-42)	-141 (-42)	-141 (-37)	-139 (-37)

Table S5. The PBE + U Schottky barriers (eV) for (a) A-stacking and (b) B-stacking $Fe_3GeTe_2/CrGeTe_3$ with different U_{eff} values (eV) of Cr_3d and Fe_3d. The dash line indicates an ohmic contact.

(a)

Fe\Cr	1	2	3	4
1	0.06	0.03	0.02	0.01
2	0.02	-	-	-
3	0.03	-	-	-
4	0.04	-	-	-

(b)

Fe\Cr	1	2	3	4
1	0.20	0.20	0.19	0.17
2	0.04	0.02	0.01	-
3	-	-	-	-
4	-	-	-	-

References

1 G. Kresse and J. Furthmüller, *Phys. Rev. B*, 1996, **54**, 11169–11186.
2 S. Grimme, S. Ehrlich and L. Goerigk, *J. Comput. Chem.*, 2011, **32**, 1456–1465.
3 S. Grimme, J. Antony, S. Ehrlich and H. Krieg, *J. Chem. Phys.*, 2010, **132**, 154104.
4 J. P. Perdew, K. Burke and M. Ernzerhof, *Phys. Rev. Lett.*, 1996, **77**, 3865–3868.
5 a. I. Lichtenstein, V. I. Anisimov and J. Zaanen, *Phys. Rev. B*, 1995, **52**, 5467–5471.
6 P. E. Blöchl, *Phys. Rev. B*, 1994, **50**, 17953–17979.
7 J. D. Pack and H. J. Monkhorst, *Phys. Rev. B*, 1977, **16**, 1748–1749.
8 V. Carteaux, D. Brunet, G. Ouvrard and G. Andre, *J. Phys. Condens. Matter*, 1995, **7**, 69–87.
9 M. A. McGuire, H. Dixit, V. R. Cooper and B. C. Sales, *Chem. Mater.*, 2015, **27**, 612–620.
10 H. J. Deiseroth, K. Aleksandrov, C. Reiner, L. Kienle and R. K. Kremer, *Eur. J. Inorg. Chem.*, 2006, 1561–1567.